VERSITA
DOI:10.2478/bile-2013-0018

Biometrical Letters
Vol. 50 (2013), No. 2, 61-80

A Bayesian model to compare vinification procedures

Federico Mattia Stefanini[1], **Ottorino-Luca Pantani**[2]

[1]Dipartimento di Statistica, Informatica, Applicazioni 'G.Parenti',
Università degli Studi di Firenze, viale Morgagni 59, I-50134 Firenze, Italia,
e-mail:stefanini@disia.unifi.it
[2]Dipartimento di Scienze delle Produzioni Agroalimentari e dell'Ambiente,
Università degli Studi di Firenze, Piazzale Cascine 28, I-50144 Firenze, Italia,
e-mail:OLPantani@unifi.it

Summary

The effects of three pre-fermentative techniques (standard procedure, cold soak pre-fermentation and cryomaceration), temperature (20 or 30°C) and saignée (with/without) on the extraction of total anthocyanins were investigated during maceration of must obtained from Sangiovese grapes. A Bayesian hierarchical model was developed to estimate time-dependent contrasts while addressing the peculiar features displayed by the experimental units (wine tanks): substantial heterogeneity among replicates, departure from low-order 'textbook' kinetics and the occasional presence of very low observations. Prior distributions of critical model parameters were elicited with the help of wine–making experts and by considering the results of previous experiments. The posterior distribution of model parameters was approximated by Markov Chain Monte Carlo simulation using JAGS software. Among the main findings, it is to be highlighted that temperature and saignée increased the total anthocyanin concentration in all the techniques, although at different times during maceration. In all the procedures the total anthocyanin gain decreased as the maceration came to an end.

Key words: semiparametric regression, outliers, MCMC, wine making, pre-fermentation treatments

1. Introduction

Flavonoids affect the colour, mouth-feel and ageability of red wines (Glories, 1988; Ribereau-Gayon and Glories, 1986). They are extracted from skins and seeds during the maceration/fermentation process (Amrani Joutei and Glories, 1995). They are phenols and include flavanols, flavonols and anthocyanins. Intensely coloured wines can be obtained through : i) pre-fermentative cold maceration, where crushed berries are kept at low temperatures for 2-5 days (Cuenat et al., 1996; Feuillat, 1997; Gerbaux, 1993; Gerbaux et al., 2002; Gordillo et al., 2010) ii) cryoextraction, where a cryogenic

liquid is kept in contact with berries for 2-4 days (Parenti et al., 2004; Couasnon, 1999).

A conclusive demonstration of the positive role of these techniques has not yet been made; in particular, many papers deal with the co-lour at the end of fermentation and do not consider its development over time. Attempts to fit plain mathematical models without considering the statistical properties of estimating procedures are provided by (Amendola et al., 2010) and (Bucic-Kojic et al., 2007), who based their work on Fick's second law, and described the evolution of total phenolic concentration during solid-liquid extraction from matrices other than must or wine. The previous models were extended in (Andrich et al., 2005) to take account of diffusion and oxidation phenomena. A class of models made by sigmoidal functions or by a linear plus exponential combination was recently proposed (Amendola et al., 2010) to describe the formation of pigmented polymers and the concentration of malvidine in must from Sangiovese grapes. A piecewise linear model for the concentration of 16 polyphenols was first proposed by (Soleas et al., 1998), as a flexible model to describe wine fermentation. Due to the lack of analysis of residuals, confidence intervals and other statistical characterizations, it remains difficult to judge the effectiveness of the above proposals in actual applications.

Longitudinal statistical models (Hedeker and Gibbons, 2006) include growth and repeated measure models in which parameters are estimated while taking account of within-subject correlation. Classical polynomial regression often uses orthogonal polynomials to model time dependence (Hedeker and Gibbons, 2006, section 5.3). Polynomial models guarantee the smoothness of estimated expected values along time, but locally varying functions may be badly estimated because data points influence the global fit of the model.

Flexible semiparametric regression models are nowadays built to describe smooth nonlinear functions by means of generalized basis functions (Ruppert et al., 2003, for a textbook presentation). This class of models may be conveniently fitted with penalized splines (Eilers and Marx, 1996), for example to avoid knots selection. In our experiment, extra model flexibility was needed due to the presence of extremely low values occurring on occasional days.

In this paper, a Bayesian hierarchical model was formulated to estimate the effect of three experimental factors, arranged in a full factorial design, on the extraction of total anthocyanins (TA) during maceration of must.

Both the probability of occurrence and magnitude of extremely low values were explicitly modelled. Tank-specific kinetics of TA and the expected value over tanks (higher hierarchical level) were estimated for each treatment. Time-dependent contrasts were calculated to compare the kinetic of each treatment against the presumably mildest one.

2. Materials and methods

In this section the experimental design and the winemaking protocol are described, together with details on laboratory equipment. The Bayesian hierarchical model is presented by introducing the likelihood function and by describing the prior distribution of model parameters.

2.1. Wine–making protocol and experimental design

The experiment was performed on Sangiovese grapes, 2010 vintage, hand picked in buckets (20 kg) at maturity in Maremma, Southern Tuscany. As the harvest proceeded through rows, a randomization procedure was used to allocate the buckets within bins (500 L), which were transported to the Consorzio Tuscania experimental winery. Each bin (destemmed-crushed berries) was randomly assigned to one of the 36 cylindrical vinification tanks (1000 L, stainless steel) which were used for the vinification. Each tank finally contained 800 L of must to be processed. A programmable control unit (Parsec s.r.l.) regulated both temperatures and pump-overs of every single tank.

A balanced full factorial experiment defined by 3 experimental factors with 3 replicates (tanks) within treatment was performed. A treatment is defined by the levels selected for each of the 3 experimental factors, which were:

- maceration, with 3 levels (traditional vinification (*Ctrl*), cold soak pre-fermentation (*CSPF*), cryomaceration (*Cryo*));
- temperature, with 2 levels (20°C or 30°C);
- saignée, with 2 levels (present or absent).

Saignée was targeted to 20% vol/weight of the total volume of the tank (1000 L). A total of 12 different treatments were considered, and the treatment *Ctrl 20°C, no saignée* was selected as the reference because experts recommended it as the mildest among those considered.

Briefly, destemmed-crushed berries for *Ctrl* were sent directly to the tanks and brought to the planned fermentation temperature. *CSPF* was

applied in the tank on the destemmed-crushed berries, lowering the temperature to 5°C immediately after filling and maintaining it for 48 hours. Cryomaceration was performed on the destemmed and drained berries using an experimental apparatus (Parsec s.r.l.) consisting of a freezing tunnel containing a stainless steel conveyor belt, on top of which some sprinklers for liquid nitrogen were installed. The contact time of the liquid nitrogen with the berries was approximately $5 - 10$ seconds, such to obtain a final temperature of the mass below 0°C, as regulated by the speed of the conveyor belt. The temperature of the flowing mass was measured and was found to be between $+7$°C and -5°C. The *Cryo*-treated berries were then crushed and added with the previously drained must.

The vinification lasted 14 days for *Cryo* and *Ctrl*, while 4 extra days were required for *CSPF*. The time was rescaled within the range $[0, 100]$ for all the treatments, thus it represents the percentage of completed maceration.

2.2. Must sampling and laboratory analyses

Sampling was performed during vinification on a daily basis just after a pumping–over. A volume of 100 ml was withdrawn from the sampling valve, labelled, and added with 400 mg of NaF to stop the fermentation process; it was then processed for chemical analyses. The UV/VIS spectra of the supernatants were recorded after centrifugation at 3840 g for 15 minutes (Agilent 8543 UV-Visible DAD spectrophotometer equipped with a 1FS peristaltic pump and a G18011A XY-auto sampler and UV-Visible ChemStation (Rev B01.01[21]) software). Total anthocyanins were determined by UV and visible spectra registered from 230 to 900 nm in a 1 cm path-length quartz flow cell. Wine samples (80 ml) were diluted with 3 ml of a solution of water:ethanol:HCl (29:70:1) by volume. The instrument was previously zeroed with this solution. The TA and non-anthocyanic flavonoids were quantified according to (Di Stefano et al., 1989) by automated macro peak integration and calculation using ChemStation software. The peak height at 280 nm was measured at the tangent baseline between the two valleys, corresponding to the absorbance of total flavonoids. More details of the analyses are given in (Buratti et al., 2007). Only the variable representing TA is considered in this paper.

2.3. A Bayesian statistical model

In this section a Bayesian hierarchical model is developed to estimate the kinetics of TA under different treatments. The semiparametric model de-

scribed below accounts for the presence of outliers, that is extraordinary small values with respect to nearby observations.

The function representing the expected value of the response (TA) is smooth and it is represented by means of B-spline bases (de Boor, 1978). Instead of looking for the optimal placement of knots, a penalized smoother is adopted by defining a suitable Bayesian prior distribution on spline parameters (Lang and Brezger, 2004; Eilers and Marx, 1996).

Let $Y(t)$ be the response variable at time t in a given tank. Among the experimental factors maceration m is labelled by integers $\{1, 2, 3\}$, temperature c by $\{1, 2\}$, and saignée s by $\{0, 1\}$. Three replicates were run for each treatment; therefore a total of 36 tanks were considered. The index $j \in \{1, 2, 3\}$ refers to the three tanks within a treatment, while an integer $i \in \{1, 2, \ldots, 12\}$ is used hereafter to denote treatments instead of using the triple of integers m, c, s.

The smooth function describing the expected value of the response variable $Y(t)$ over time was decomposed into a function $\mu(t)$, which is the expected value of the treatment, plus a function related to the departure of a tank from the expected value of its own treatment, formally written as:

$$E[Y_{i,j}(t)] = \mu_i(t) + \alpha_{i,j}(t) \tag{1}$$

where $\alpha_{i,j}(t)$ is the time-dependent effect due to tank j, that is the departure of a given tank from the expected value $\mu_i(t)$ of treatment i. The function $\alpha_{i,j}(t)$ for tank j is also assumed to be smooth and to be well represented by spline bases.

At each sampling time (index t omitted) $Y_{i,j} = E[Y_j \mid m, c, s] + \epsilon_j$, with the error $\epsilon_j \sim N(0, \sigma^2_{i,j})$, thus such variance depends both on treatment and tank within treatment; errors are assumed to be independent and to follow a normal distribution.

An estimate $\hat{\mu}_i(t)$ of the unknown $\mu_i(t)$ is the kinetic law inferred using three tanks and it is also exploited to compare two different treatments. The pointwise difference among expected values is the natural extension of ANOVA contrasts to time-dependent effects:

$$\delta_{i,k}(t) = \mu_i(t) - \mu_k(t) \tag{2}$$

with i the test treatment and $k \neq i$ the reference treatment. For example, a flat estimated function $\hat{\delta}_{i,k}(t)$ which is equal to zero over time indicates no differences between test and reference treatments at every time point t. A flat but not null estimated function $\hat{\delta}_{i,k}(t) \neq 0$ indicates that the two

considered kinetics differ by the same constant value at every time point t. Estimated time-dependent contrasts are shown in Figure 5.

2.3.1. B-spline bases

B-splines are built from polynomial pieces which are joined at selected values of time, called knots, here the % of elapsed days since the start of maceration. The computation with B-splines is detailed in (de Boor, 1978) and in (Dierckx, 1995).

B-splines show no boundary effects and are computationally quite tractable if compared with other classes of splines. Note that the derived models still depend on parameters, as it happens in regression, but they are not straightforwardly interpretable. Nevertheless, B-splines provide a way to represent a locally varying smooth function of time, here expected values of TA concentration. The general properties of B-splines can be found in (Eilers and Marx, 1996).

Given a grid of points at selected time values, B-splines are matrices representing generalized bases of a linear model:

$$\mu_i(t) = \boldsymbol{M}_i \, \boldsymbol{\beta}_i \tag{3}$$

thus the smooth function for the expected value of a treatment is described through $\boldsymbol{M}_i$. In a similar way, the smooth function for the departure of a given tank from the expected value is also represented by B-splines:

$$\alpha_{i,j}(t) = \boldsymbol{A}_{i,j} \, \boldsymbol{\beta}_{i,j} \tag{4}$$

with j the index of tanks. The observations performed at given time points may be decomposed as detailed in the equation below if the same basis functions are used within treatment, that is $\boldsymbol{A}_{i,j} = \boldsymbol{M}_i$:

$$\boldsymbol{y}_{i,j} = \boldsymbol{M}_i \, \boldsymbol{\beta}_i + \boldsymbol{M}_i \, \boldsymbol{\beta}_{i,j} + \boldsymbol{\epsilon}_{i,j} \tag{5}$$

where i refers to treatments, j to tanks within treatment and with $\boldsymbol{y}_{i,j}$ the vector of responses (TA).

2.3.2. The likelihood function

In equation (5) a decomposition is provided which is able to address the needs described in the introduction: heterogeneity among replicates and flexibility in the shape of kinetics. The model accommodates the main features found in this experiment and in similar contributions of the literature: the lack of an actual horizontal upper asymptote, the variability

in the shape of the kinetic within replicates and the lack of a standard 'textbook' shape for the expected value of TA over time.

Occasionally there appear outliers, characterized by extraordinary small values with respect to nearby observations (Figure 4). The availability of three replicates for each treatment and the huge size of such decreases, even down to one half of the expected value, allowed the detection of outliers by visual inspection (about 5-10% of the observations, Figure 4). Outliers may be included in the analysis if the model properly takes into account their features. Such a rigorous statistical approach makes it possible to estimate the proportion of outliers occurring within a tank. An extension of equation (5) was obtained by generalizing the expected value of the response:

$$E[\ \boldsymbol{Y}_{i,j}] = (\ \boldsymbol{M}_i\ \boldsymbol{\beta}_i + \ \boldsymbol{M}_i\ \boldsymbol{\beta}_{i,j}) \cdot\ \boldsymbol{\eta}_{i,j} \tag{6}$$

where $\boldsymbol{\eta}_{i,j}$ is a $K_i \times 1$ vector in which each element is in the open set $(0, 1)$ if it corresponds to an outlier, otherwise it is equal to 1 (regular observation).

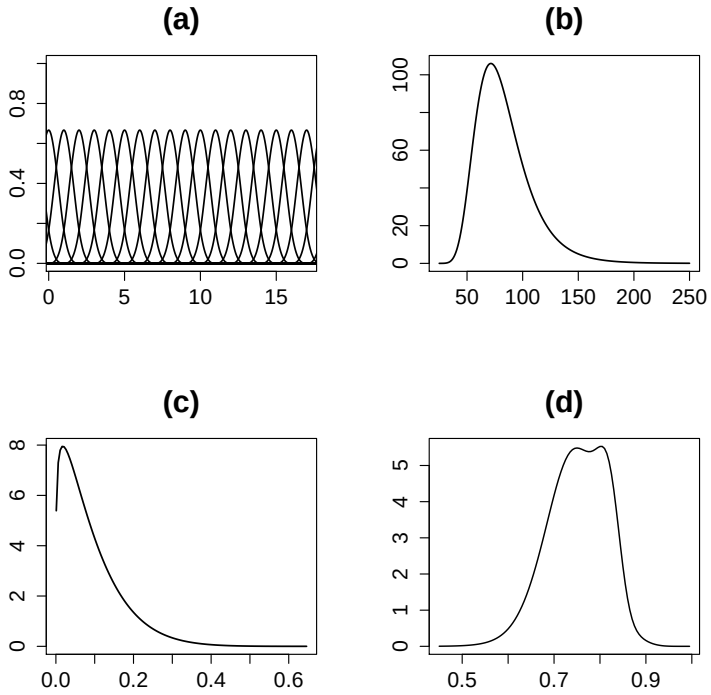

Figure 1. Splines and prior distributions (a) Example of B-spline bases of degree 3 (order 4) (b) Prior distribution for the variance of the response (c) Prior distribution for the probability that an observation is an outlier (d) Prior distribution for the magnitude $\eta_{i,j,k}$ of an outlier

The likelihood function for all the observations is therefore:

$$p(\ \boldsymbol{y}_{i,j}\ |\ \ \boldsymbol{\theta}) = \prod_{i=1}^{12} \mathcal{MN}\Big(\ [\ \boldsymbol{M}_i\ \boldsymbol{\beta}_i + \ \ \boldsymbol{M}_i\ \boldsymbol{\beta}_{i,j}] \cdot\ \boldsymbol{\eta}_{i,j}, \quad \boldsymbol{\Sigma}_{i,j}\Big) \tag{7}$$

where $\mathcal{MN}()$ stands for multivariate normal distribution and with $\boldsymbol{\Sigma}_{i,j}$ the diagonal variance-covariance matrix $\boldsymbol{\Sigma}_{i,j} = \sigma^2_{\epsilon,i,j}\ \boldsymbol{I}$; vector $\boldsymbol{\theta}$ contains all model parameters of the likelihood function.

2.3.3. Bayesian elicitation of prior distributions.

The full specification of a Bayesian model is made by assigning a probability distribution to all unknowns, such as model parameters. The elicitation consists of quantifying the degree of belief that an expert associates to the possible values taken by each unknown model parameter, for example by reasoning on equipment features or about results of previous experiments. For a comprehensive account on elicitation see (Garthwaite et al., 2005).

Let $\sigma^2_{\epsilon,i,j}$ be the 36 variances of residuals in different treatments. The initial (prior) distribution of the precision, that is the inverse of the variance, is $\sigma^{-2}_{\epsilon,i,j} \sim \mathcal{G}(15, 1000)$, where $\mathcal{G}$ indicates the Gamma distribution (Figure 1b): it is clear that values of variance below 10 or above 200 are not a-priori plausible in our model.

The model term $\boldsymbol{M}_i\ \boldsymbol{\beta}_i$ in equation (7) describes a smooth function for the expected value of a regular TA value (it is not an outlier). To avoid the explicit selection of knots, 21 equispaced points were selected from the interval $[0, 1]$ on the time axis and stochastic constraints on the elements of vector $\boldsymbol{\beta}_i$ were posed (Eilers and Marx, 1996). Let $\beta_{i,r}$ be the element in position r of vector $\boldsymbol{\beta}_i$, then:

$$\beta_{i,r+1} \ \sim\ \mathcal{N}(\beta_{i,r}, \sigma^2_{M,i}) \tag{8}$$

$$\beta_{i,1} \ \sim\ \mathcal{N}(0, 0.00001) \tag{9}$$

$$\sigma^{-2}_{M,i} \ \sim\ \mathcal{G}(0.001, 0.001) \tag{10}$$

where r is the index spanning pairs of subsequent times and $\mathcal{N}()$ is the univariate normal distribution. $\mathcal{G}()$ indicates the Gamma distribution. Note that the degree of similarity existing between pairs of subsequent elements $\beta_{i,r}, \beta_{i,r+1}$ is regulated by the unknown parameter $\sigma^2_{M,i}$, with its final distribution determined by the results of the experiment.

A similar definition holds for tank-specific functions representing depar-

tures from the treatment mean:

$$\begin{aligned} \beta_{i,j,r+1} &\sim \mathcal{N}(\beta_{i,j,r}, \sigma^2_{A,i,j}) && (11)\\ \beta_{i,j,1} &\sim \mathcal{N}(0, 0.00001) && (12)\\ \sigma^{-2}_{A,i,j} &\sim \mathcal{G}(0.001, 0.001) && (13) \end{aligned}$$

with r the index spanning pairs of subsequent times.

The initial distribution for the probability of being an outlier at a given point in time is shown in Figure 1c, which is a Beta probability density function:

$$\pi_{F,i} \sim \mathcal{B}(1.2, 12) \tag{14}$$

therefore the expected value is equal to 0.1: it is believed that one out of ten observations on average is an outlier. Bernoulli Boolean variables $W_{i,j,k} \sim (1-\pi_{F,i})^{1-w_{i,j,k}} + \pi_{F,i}^{w_{i,j,k}}$, with $i = 1, \ldots, 12, j = 1, 2, 3, k = 1, 2, \ldots, K_i$ are unobserved indicator variables taking value 1 if the observation $y_{i,j,k}$ is an outlier, zero otherwise. They are assumed to be independent over tanks (index j) and treatments (index i). Note that only extreme outliers are detected by visual inspection without uncertainty, i.e. all observations being extremely small with respect to their neighbours.

Given that an observation $y_{i,j,k}$ is an outlier, that is $W_{i,j,k} = 1$, the magnitude of its reduction is unknown and it is represented by parameter $\eta_{i,j,k}$, that is the ratio of original-to-outlying mean values. For a regular observation, $W_{i,j,k} = 0$, the ratio is :

$$p(\eta_{i,j,k} \mid W_{i,j,k} = 0) = I_1(\eta_{i,j,k}) \tag{15}$$

thus $W_{i,j,k} = 0$ causes $\eta_{i,j,k}$ to have a degenerate distribution at the point $\eta_{i,j,k} = 1$. For outliers, $W_{i,j,k} = 1$, the probability density function indicating the amount of reduction was elicited as a mixture of Beta distributions (Figure 1d):

$$\begin{aligned} p(\eta_{i,j,k} \mid W_{i,j,k} = 1) = \; & 0.275\ \mathcal{B}(8, 24) + 0.55\ \mathcal{B}(17.5, 48) + \\ & +0.175\ \mathcal{B}(45, 200) \end{aligned} \tag{16}$$

where $\mathcal{B}()$ stands for the Beta distribution. Elements within $\boldsymbol{\eta}_{i,j}$ are assumed to be independent, that is $p(\boldsymbol{\eta}_{i,j} \mid \boldsymbol{W_{i,j}}) = \prod_k p(\eta_{i,j,k} \mid W_{i,j,k})$, with $\boldsymbol{W_{i,j}} = \{W_{i,j,k} : k = 1, 2, \ldots, K_i\}$. It is also assumed that vectors $\boldsymbol{\eta}_{i,j}$ are independent.

3. Results and discussion

This section opens with a description of the Bayesian computations and their quality. Then the marginal posterior distribution of some model parameters is described. Finally the expected value of kinetics under different treatments is presented, together with the estimated time-dependent contrasts against the reference treatment.

All the computations were performed with the R software (Team, 2010) using libraries like lattice (Sarkar, 2008) and rjags (Plummer, 2003).

3.1. Model fitting

The posterior distributions of model parameters and the expected value of functions of some model parameters were obtained by Markov Chain Monte Carlo simulation (Robert and Casella, 2010) using the JAGS software (Plummer, 2003).

At first, one simulation comprising all 12 treatments was performed. The selection of a bad starting point in combination with large error variances within tank drove the simulation of simpler models far from convergence. Similar effects were observed reducing the number of parameters related to splines in different treatments. One explanation of these results is related to the presence of different levels of noise in different tank-treatments, so that a satisfactory model fit was obtained only by tank–specific parameters. It was therefore decided to run 12 separated simulations, one for each treatment. The convergence of Markov chains was improved remarkably by imposing the condition that at each time t, the effects are subject to a sum-to-zero constraint $\sum_j \alpha_j(t) = 0$.

The starting points of each Markov chain were randomly generated around the maximum likelihood point estimate of a simplified version of the Bayesian model. The initial burn-in of chains was 25000 steps, while 100000 iterations were saved after thinning by 10 for each chain. The final output of 10000 sampled values for each chain was processed with standard post-simulation numerical diagnostics (Brooks and Gelman, 1997; Cowles and Carlin, 1996), and diagnostic plots, like autocorrelations and cross-correlations. Overall, the quality of chains output seemed almost always good. By repeating MCMC runs several times it was possible to assess the effect of starting points on the simulation, and the odd behaviour observed when running the initial simpler model disappeared.

After model fitting, the difference between observed values and expected values from the marginal posterior distribution given a day-tank pair was

calculated to plot quantile-quantile relations (not shown). No obvious violation of the assumption of normality was found in any treatment.

3.2. Posterior distribution of model parameters and estimated kinetics

Equation (14) represents the prior distribution of π_F, the probability of being an outlier for a given treatment-tank combination. In Figure 2, the marginal posterior distribution given a treatment is shown. The mode of the posterior distribution is always below 0.1 and it is closest to 0.01 in the following treatments: *Ctrl 20 °C saignée*, *Ctrl 30 °C saignée*, *Ctrl 20 °C no saignée*, *CSPF 20 °C saignée*. Treatments have an impact on the probability of observing an outlier.

Indicator variables $W_{i,j,k}$ in treatment i, tank j and day k, are affected by uncertainty: it is not known where outliers are located along time. The marginal posterior distribution of an indicator $W_{i,j,k}$ summarizes the probability that a given observation is effectively an outlier (Figure 3).

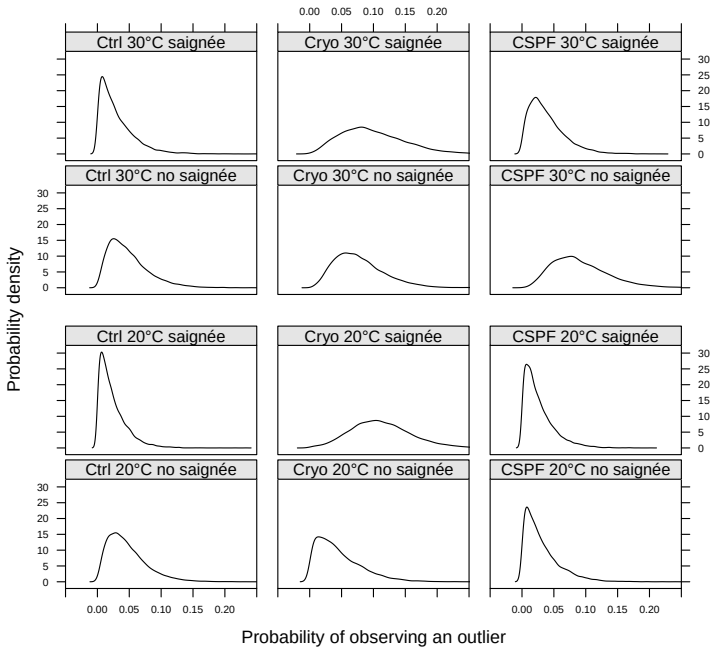

Figure 2. Final distributions. Marginal posterior probability density functions of observing an outlier in a given treatment

The presence of outliers in a treatment-tank-day may be extremely evident in almost constant regions of the kinetic, like in the kinetic of tank 3 under treatment *Cryo* $30°C$ *saignée* (Figure 4), but it may be difficult to detect outliers elsewhere without a formal model, for example in tank 1 of treatment *Cryo* $20°C$ *saignée*. The expected values of $W_{i,j,k}$ (Figure 2) are grouped by treatment, with tanks labelled as (1), (2) or (3). An unanticipated result is that outliers are almost absent in just three treatments, (*Ctrl* $30°C$ *saignée*, *Ctrl* $20°C$ *saignée*, *CSPF* $20°C$ *saignée*), and that such small observations are typically asymmetrically distributed among tanks under the same treatment (for example *Cryo* $20°C$ *saignée*). Further investigations are needed to fully understand the outlier generating process.

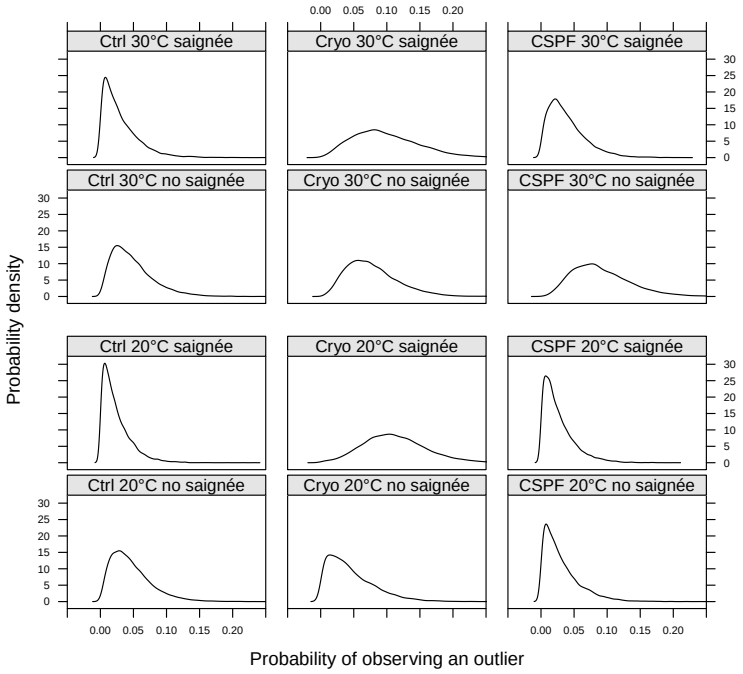

Figure 3. Estimated posterior probability of having observed an outlier in a given tank-day. Tanks within treatments are labelled with bracketed integers

The estimated kinetics of TA under different treatments are shown in Figure 4. For each time point of a dense grid defined on $[0, 100]$ the expected value and the 95% credible interval were calculated using the final distributions of model parameters.

A general feature of the estimated kinetics is smoothness with respect to time, despite the presence of perceptible departures of the tank kinetics from the smoothed treatment estimate. Other general features include the departure of estimated kinetics from the plateau in late days, where the kinetic may decrease, as in treatments *Ctrl* 30° *C saignée* and *CSPF* 30° *C no saignée*, or be still increasing, as in *CSPF* 20° *C saignée* and *Cryo* 20° *C no saignée*. Treatments made by *CSPF* are notable for an initial steady or decreasing behaviour, which is due to the nature of the treatment itself.

The estimated kinetics do not typically conform to standard laws like the sigmoid function, with the exception of treatment *Ctrl* 20° *C saignée*. Nevertheless, even in this case, our model is able to properly estimate the kinetic without knowing and excluding outliers (for example, tank 3 of Figure 4).

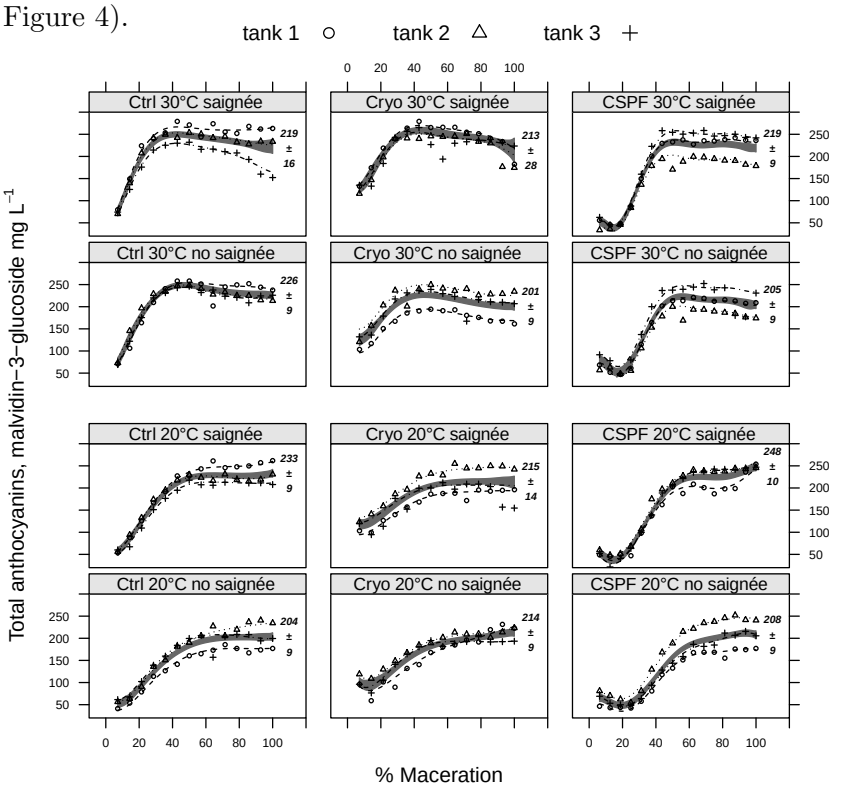

Figure 4. Kinetics of total anthocyanins during maceration. Within each panel, points represent daily observed values and the dashed lines are the (estimated) expected value for each tank. The grey region indicates the 95% point-wise credible intervals of expected values. The figures indicate the TA concentration at the end of maceration

The estimated kinetics of each treatment were exploited to obtain time-dependent contrasts (Figure 5), using marginal distributions of contrasts defined on a dense grid of time points. In the present study the mildest treatment (*Ctrl* 20°*C no saignée*) was chosen as reference, although any other choice would have been possible due to the full generality of the model. Minimum and maximum values of a contrast are decorated with numerical values to better appreciate their magnitude. Dotted lines define pointwise 95% credible intervals around the estimated expected value of the time-dependent contrast.

The dashed and straight horizontal line at zero is the reference of no effect between a treatment and the considered reference. Therefore the contrast *Ctrl* 20°*C no saignée* bottom left is horizontal and without uncertainty because the tested and reference kinetics are equal.

As regards the final concentration of anthocyanins, the top treatment is *CSPF* 20°*C saignée*, which is equal to 45 ± 13. Treatment *Ctrl* 20°*C saignée* is almost constant but above the reference treatment, due only to the presence of saignée. Other contrasts including *CSPF* show a test treatment which is late with respect to the control, but it later recovers and the contrast remains well above zero.

3.3. Effects of maceration, temperature and saignée

3.3.1. Ctrl

The leftmost column in Figure 3 shows trends similar to a 1^{st} order kinetic reaction with asymptote, but at 30 °C there is also a decrease in concentration towards the end of maceration. The differences between procedures and *Ctrl 20 °C saignée* are shown in Figure 4. All the *Ctrl* procedures show significant increases in TA concentration, which are functions of both temperature and saignée. The absolute value of the gain increases with temperature and the presence of saignée. In the most radical procedure (*Ctrl 30 °C saignée*) there is a gain of 109 mg L^{-1} at 27% of maceration, i.e. the concentration almost doubled with respect to the reference (Figure 4). At the end of the maceration the order is exactly reversed, the less drastic procedure *Ctrl 20 °C saignée* being able to yield a gain of 30 mg L^{-1}. The final outcome of the systems seems to be resilient to the conditions imposed by the procedures: the more TA was extracted at the beginning, the less TA remained at the end.

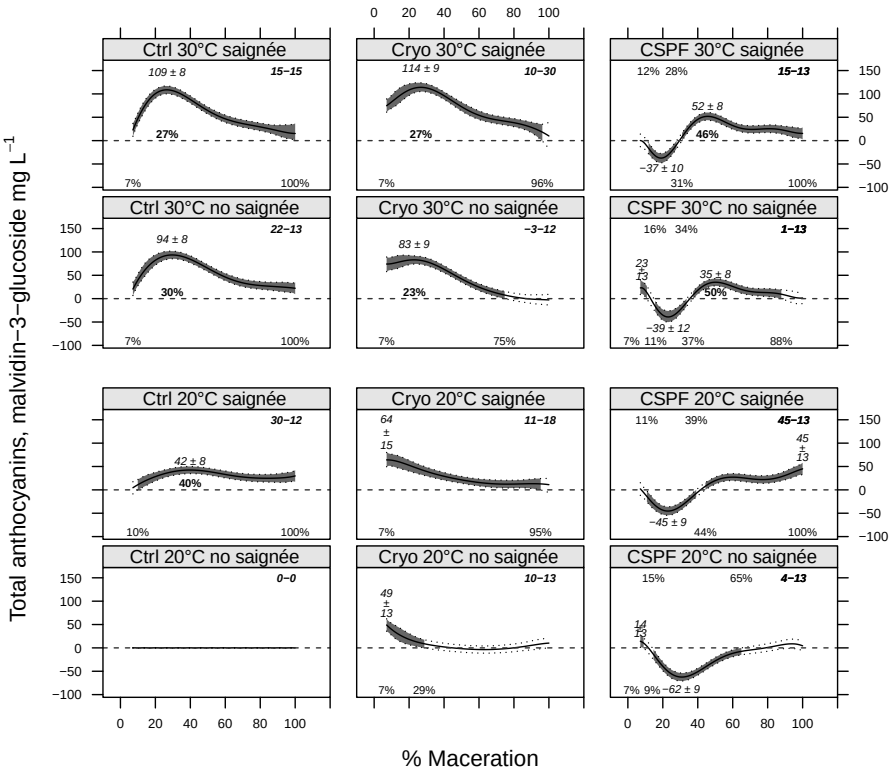

Figure 5. Time-dependent contrasts between pairs of treatment kinetics estimated on three tanks each. The dashed horizontal line indicates no effect between the tested treatment and *Ctrl* 20°C no saignée (reference). The area between the two lines (95 % credible interval) is shaded if there is a significant difference between the reference and the treatment. The figures expressed in % on the top/bottom define the time interval in which the credibility interval does not include zero. Minimum and maximum values are labelled both with numerical values ± credible interval and with % of maceration near the dashed line. The bold italic figures on top right indicate the final value minus the lower credible interval at the end of maceration

3.3.2. *Cryo*

No reference dealing with *Cryo* can be found in the literature except (Parenti et al., 2004), where kinetics are not reported. The shape of the kinetic is exponential-like (Figure 5) but with a less pronounced curvature than observed for *Ctrl*. The temperature and saignée being constant, no significant differences were found between *Cryo* and *Ctrl* (time-dependent contrasts not reported). The central column in Figure 5 shows that the gain is important at the early stage of maceration and that the absolute value of gain

increases with temperature and with saignée. At the end of maceration this gain is lost for *Cryo* treatments regardless of temperature or saignée. The shape of the gain over time is similar to that already observed for *Ctrl*; the less drastic procedure seems able to achieve the greatest gain at the end of maceration.

3.3.3. *CSPF*

The initial phase was not monitored on the Tempranillo variety with a *CSPF* held at 5-8°C for 8 days (Gordillo et al., 2010). An exponential-like shape in the same phase was monitored on the Shiraz variety, where *CSPF* was held at 15 °C for 6 days (Gómez-Míguez et al., 2007). Both authors recorded an indubitable increase (about +100-200 mg L^{-1}) of TA concentration with respect to traditional vinifications held at 25°C, both at the beginning and at the end of tumultuous fermentation. Reynolds et al. (2001) on investigating the effect of *CSPF* on Shiraz at 2°C for one or ten days, found smaller increases in TA concentration, in the order of 50-70 mg L^{-1}, which is also the range we observed (Figure 5). Other results on *CSPF* (Gerbaux, 1993; Feuillat, 1997; Gerbaux et al., 2002) confirm a rapid decrease in the anthocyanins extracted early and a lower final concentration of these molecules as compared with other extraction procedures. Due to the heterogeneous nature of the experimental conditions reported in the literature, is not possible to draw conclusive results. In the present experiment, the temperature of *CSPF* was kept at 5°C, a level low enough to reduce to a minimum the spontaneous fermentation activity before the inoculation of the selected yeast. The low temperature is possibly the main responsible for the lack of extraction of TA in the first 30-40 % of maceration for *CSPF* (Figure 4). The delay in extraction is a function of the combination of temperature and saignée, since it is maximum at the less drastic conditions (65% at 20 ° C no saignée) and becomes 31% at 30 °C saignée. Later on, when the temperature is raised, the rapid increase of TA is probably a consequence of the cold soak, which may have weakened the cell walls of berries. This hypothesis is consistent with the results obtained by (Andrich et al., 2005) who reported a decrease in the rates of anthocyanins diffusion in the liquid phase on decreasing the temperature. (Sacchi et al., 2005) reports that for cold soak "the rationale offered is that aqueous extraction improves wine color". This early aqueous extraction, as demonstrated here, seems not to occur in TA on Sangiovese at 5°C. From the review of the literature we therefore hypothesize that the gain in TA

concentration is only possible when the temperature during cold soak is kept at 10-15 °C, where faster and more effective biotic and enzymatic reactions are most likely to occur. On the other hand, the reduction/elimination of unwanted spontaneous fermentations could not easily be achieved in these warmer conditions. The time-dependent contrasts in Figure 5 show that for *CSPF* there is a small gain, but that this gain is quite stable along the whole maceration. *Ctrl* and *Cryo*, even if they show a remarkable gain increase at the beginning, later anyway have a decrease. Also for *CSPF*, the less drastic procedure allow a final gain of 45 mg L^{-1}.

3.3.4. *Temperature of fermentation*

The fairly large number of studies, carried out on different cultivars, have generally established that higher fermentation temperatures increase the colour and anthocyanin content of wines (Gao et al., 1997; Harbertson et al., 2008; Reynolds et al., 2001). The present experiment indicates that this gain is remarkable during fermentation and reaches a maximum in the first half/third of the process (Figure 5), but it also indicates that the maximum gain is observed at the end with lower temperature. As one of the aims in the vinification of Sangiovese is colour extraction and stabilization, higher temperatures are not recommended. Undoubtedly the crucial issue here is not to focus on the conditions/techniques, but rather on methods to avoid/reduce the decay of gain which is visible in all the procedures.

3.3.5. Saignée

The present results agree with those reported in literature where a larger extraction is found (Gerbaux, 1993; Zamora et al., 1994). Saignée enhances the gain for all procedures, including the higher fermentation temperature.

4. Conclusions

The Bayesian model described in this work made possible a comparison of treatments regardless of the presence of both outliers and tank heterogeneity. Uncertainty in the estimates of kinetics and time-dependent contrasts were quantified by Markov Chain Monte Carlo simulation despite the limited sample size, without resorting to asymptotic approximations. Indeed elicited prior distributions of model parameters entered into the inferential machinery but we see this as a bonus for the regularization effect exerted on estimation in such a complex model. An advantage of the hierarchical formulation is

the possibility of borrowing statistical strength about parameters of similar treatments, an issue that deserves further attention in future work.

Further research is required on the chemical side of this work because a clear explanation of the outlier generating process is still to be achieved. Analytical lab measurements were repeated for each outlying observation and its time neighbours: recorded values were always confirmed. Sample corruption or lack of proper manipulation was considered unlikely after reviewing the recorded equipment setup and field and lab notes. Analytical measurements repeated after a few hours, a week after collection and one month later always confirmed the initial measurements. We are reasonably confident of the absence of manipulation or analytical errors, and for this reason we developed a model which captured some aspects of the outlier generating process and which might be useful in monitoring these features in future experiments. A hypothesis to be considered in future work concerns the temporary unavailability of TA in the form that is detected by our laboratory protocols.

Acknowledgments

The authors wish to thank Stefano Benedettelli (DipSA) for the experimental setup; Alessandro Parenti (DIAF) and his staff (Silvia Spinelli, Piernicola Masella, and Lorenzo Nannucci) for their assistance and expertise with the equipment for cryoextraction and database interrogations; Manuel Pieri and his staff for the huge work done in the wine cellar; Lisa Granchi, Paola Domizio, and Cristina Romani (Di.B.A.) for microbiological advices and assistances; and Federico Valori, Paola Arfaioli and Irene Lozzi for assistance in preparing the samples and UV-visible measurements. Consorzio Tuscania is acknowledged for partial support of this project.

References

Amendola D., De Faveri D., Spigno G. (2010): Grape marc phenolics: extraction kinetics, quality and stability of extracts. Journal of Food Engineering 97(3): 384–392.

Amrani Joutei K., Glories Y. (1995): Tanins at anthocyanes: localisation dans la baie de raisin et mode d'extraction. Revue Francaise d'Oenologie 153: 28–31.

Andrich G., Zinnai A., Venturi F., Fiorentini F. (2005): A tentative mathematical model to describe the evolution of phenolic compounds during the maceration of Sangiovese and Merlot grapes. Italian journal of food science 17: 45–58.

Brooks S., Gelman A. (1997): General methods for monitoring convergence of iterative simulations. Journal of Computational and Graphical Statistics 7: 434–455.

Bucic-Kojic A., Planinic M., Tomas S., Bilic M., Velic D. (2007): Study of solid-liquid extraction kinetics of total polyphenols from grape seeds. Journal of Food Engineering 81(1): 236–242.

Buratti S., Ballabio D., Benedetti S., Cosio M. (2007): Prediction of Italian red wine sensorial descriptors from electronic nose, electronic tongue and spectrophotometric measurements by means of Genetic Algorithm regression models. Food Chemistry 100(1): 211–218.

Couasnon M.B. (1999): Une nouvelle technique: la maceration préfermentaire à froid – Extraction à la neige carbonique. Premier partie: Rèsultats oenologiques. Revue des Oenologues 92: 26–30.

Cowles M., Carlin B. (1996): Markov Chain Monte Carlo convergence diagnostics: a comparative study. Journal of the American Statistical Association 91: 883–904.

Cuenat P., Lorenzini F., Bregy C., Zufferey E. (1996): La macération préfermentataire à froid du Pinot noir. Aspects technologiques et microbiologiques. Revue suisse de viticulture arboriculture horticulture 28: 259–265.

de Boor C. (1978): A Practical Guide to Splines, number 27 *in* Applied Mathematical Sciences Series. New York: Springer-Verlag.

Di Stefano R., Cravero M. C., Gentilini M. (1989): Metodi per lo studio dei polifenoli dei vini. L'enotecnico 5: 83–89.

Dierckx P. (1995): Curve and Surface Fitting with Splines. Oxford: Oxford University Press. ISBN13: 9780198534402 ISBN10: 019853440X.

Eilers P.H.C., Marx B.D. (1996): Flexible smoothing with B-splines and penalties. Statistical Science 11: 89–121.

Feuillat M. (1997): Vinification du Pinot noir en Bourgogne par macération préfermentaire à froid. Revue des Oenologues 82: 29–31.

Gao L., Girard B., Mazza G., Reynolds A.G. (1997): Changes in anthocyanins and color characteristics of Pinot Noir wines during different vinification processes. Journal of Agricultural and Food Chemistry 45(6): 2003–2008.

Garthwaite P.H., Kadane J.B., O'Hagan A. (2005): Statistical methods for eliciting probability distributions. Journal of the American Statistical Association 100: 680–701.

Gerbaux V. (1993): Etude de quelques conditions de cuvaison susceptibles d'augmenter la composition polyphenolyque des vins de pinot noir. Revue des Oenologues 69: 15–18.

Gerbaux V., Vuittenez B., Vincent B., L'Heveder A. (2002): Macerazione prefermentativa a freddo e macerazione finale a caldo su Pinot nero in Bourgogne, http://www.infowine.com 4: 1–5. ISSN 1826-1590.

Glories Y. (1988): Anthocyanins and tannins from wine: organoleptic properties. Progress in clinical and biological research 280: 123–34.

Gómez-Míguez M., González-Miret M. L., Heredia F. J. (2007): Evolution of colour and anthocyanin composition of Syrah wines elaborated with prefermentative cold maceration. Journal of Food Engineering 79(1): 271–278.

Gordillo B., López-Infante M.I., Ramìrez-Pérez P., Gonzàlez-Miret M.L., Heredia F.J. (2010): Influence of prefermentative cold maceration on the color and anthocyanic copigmentation of organic Tempranillo wines elaborated in a warm climate. Journal of Agricultural and Food Chemistry 58(11): 6797–6803. PMID: 20455543.

Harbertson J.F., Hodgins R.E., Thurston L.N., Schaffer L.J., Reid M.S., Landon J.L., Ross C.F., Adams D.O. (2008): Variability of tannin concentration in red wines. American Journal of Enology and Viticulture 59(2): 210–214.

Hedeker D., Gibbons R. (2006): Longitudinal Data Analisys, Wiley Series in Probability and Statistics. Hoboken, New Jersey: John Wiley and Sons.

Lang S., Brezger A. (2004): Bayesian P-Splines. Journal of Computational and Graphical Statistics 13(1): 183–212.

Parenti A., Spugnoli P., Calamai L., Ferrari S., Gori C. (2004): Effects of cold maceration on red wine quality from Tuscan Sangiovese grape. European Food Research and Technology 218: 360–366. 10.1007/s00217-003-0866-1.

Plummer M. (2003): JAGS: A program for analysis of Bayesian graphical models using Gibbs sampling, Proceedings of the 3rd International Workshop on Distributed Statistical Computing (DSC 2003). http://www-ice.iarc.fr/martyn/software/jags/

Reynolds A., Cliff M., Girard B., Kopp T.G. (2001): Influence of fermentation temperature on composition and sensory properties of Semillon and Shiraz wines. American Journal of Enology and Viticulture 52(3): 235–240.

Ribereau-Gayon P., Glories Y. (1986): Phenolics in grapes and wines, in 6th Australian Wine Industry Technical Conference, ed. T. Lee, Australian Wine Industry Technical Conference Inc., Adelaide, Australia: 247–256.

Robert C., Casella G. (2010): Introducing Monte Carlo Methods with R, number 27 in Use R!. Heidelberg: Springer-Verlag.

Ruppert D., Wand M., Carroll R. (2003): Semiparametric Regression. Cambridge: Cambridge University Press.

Sacchi K.L., Bisson L.F., Adams D.O. (2005): A review of the effect of winemaking techniques on phenolic extraction in red wines. American Journal of Enology and Viticulture 56(3): 197–206.

Sarkar D. (2008): Lattice: multivariate data visualization with R. New York: Springer. ISBN 978-0-387-75968-5. http://lmdvr.r-forge.r-project.org

Soleas G.J., Tomlinson G., Goldberg D.M. (1998): Kinetics of polyphenol release into wine must during fermentation of different cultivars. Journal of Wine Research 9: 27–41.

Team R.D.C. (2010): R: a language and environment for statistical computing. ISBN 3-900051-07-0. http://www.R-project.org/

Zamora J.B., Luengo G., Margalef P., Magrina M., Arola L. (1994): Nota: Efecto del sangrado sobre el color y la composicion en compuestos fenolicos del vino tinto. Revista Española de Ciencia y Tecnología de Alimentos 34: 663–671.